The Interactions of Cyanobacterial Cytochrome c_6 and Cytochrome f, Characterized by NMR*⑤

Peter B. Crowley‡, Antonio Díaz-Quintana§, Fernando P. Molina-Heredia§, Pedro Nieto§, Martin Sutter¶, Wolfgang Haehnel¶, Miguel A. De la Rosa§, and Marcellus Ubbink‡∥

From the ‡Leiden Institute of Chemistry, Leiden University, Gorlaeus Laboratories, P. O. Box 9502, 2300 RA Leiden, The Netherlands, §Centro de Investigaciones Científicas Isla de la Cartuja, Universidad de Sevilla y Consejo Superior de Investigaciones Científicas, Américo Vespucio s/n, 41092 Sevilla, Spain, and ¶Institut für Biologie II, Albert-Ludwigs-Universität Freiburg, Schänzlestrasse 1, D-79104 Freiburg, Germany

During oxygenic photosynthesis, cytochrome c_6 shuttles electrons between the membrane-bound complexes cytochrome bf and photosystem I. Complex formation between *Phormidium laminosum* cytochrome f and cytochrome c_6 from both *Anabaena* sp. PCC 7119 and *Synechococcus elongatus* has been investigated by nuclear magnetic resonance spectroscopy. Chemical-shift perturbation analysis reveals a binding site on *Anabaena* cytochrome c_6, which consists of a predominantly hydrophobic patch surrounding the heme substituent, methyl 5. This region of the protein was implicated previously in the formation of the reactive complex with photosytem I. In contrast to the results obtained for *Anabaena* cytochrome c_6, there is no evidence for specific complex formation with the acidic cytochrome c_6 from *Synechococcus*. This remarkable variability between analogous cytochromes c_6 supports the idea that different organisms utilize distinct mechanisms of photosynthetic intermolecular electron transfer.

Electron transport between the membrane-bound complexes cytochrome bf and photosystem I (PSI)[1] is maintained by mobile electron carriers. In plants, this task is fulfilled by plastocyanin (Pc), whereas cytochrome c_6 (cytc_6) is the only carrier in certain cyanobacteria. There also exist eukaryotic algae and cyanobacteria, which have the capacity to replace Pc with cytc_6 under copper-depleted conditions (1). Recently, a cytc_6-like protein has been discovered in the thylakoid lumen of *Arabidopsis* (2, 3). Despite being evolutionarily unrelated, Pc and cytc_6 perform equivalent tasks with common reaction partners. This functional convergence suggests that similar interaction properties exist for both proteins. Not surprisingly, Pc and cytc_6 have comparable redox potentials of around 350 mV. Furthermore, both proteins provide similar recognition information, demonstrated by the parallel variation of their isoelectric points, being acidic in green algae while ranging from acidic to basic in cyanobacteria (1, 4, 5).

To date there has been a considerable amount of kinetic and mutational analysis of the electron transfer reaction between both Pc and cytc_6 and their partner PSI (6–11). A hierarchy of mechanisms for interprotein electron transport has emerged from this work. Reduction of PSI by Pc or cytc_6, isolated from different organisms, can follow an oriented collision mechanism (type I), a two-step mechanism requiring complex formation (type II), or a complex formation with rearrangement of the interface before electron transfer occurs (type III). A remarkable homology between the arrangement of charged and hydrophobic recognition patches on the surfaces of Pc and cytc_6 has also been revealed (12, 13). In particular, a conserved arginine found in cyanobacterial Pc and cytc_6 was shown to be critical for bimolecular association with PSI (9).

Two structures of the cyt$f$-Pc complex from plant (14) and cyanobacterial (15) sources have been determined. A combination of charged and hydrophobic patches defines the complex interface between turnip cyt$f$ and spinach *Pc*. In contrast, the complex from *Phormidium laminosum*, a thermophilic cyanobacterium, was found to be predominantly hydrophobic. At present there are no kinetic or structural data for the interaction of cytc_6 and cyt$f$. Although mutagenesis studies have identified key residues for the reaction with PSI, there is no knowledge of the interaction site involved with cyt$f$.

To address the question of molecular recognition in cytc_6, we have investigated complex formation with cyt$f$ using heteronuclear NMR. We have aimed to identify the surface features involved in complex formation and to draw comparisons with cytc_6-PSI interactions. Two cyanobacterial variants of cytc_6 (Fig. 1), the basic protein from *Anabaena* sp. PCC 7119 (pI 9.0) and the acidic protein from *Synechococcus elongatus* (pI 4.8), have been studied. In this way, the role of electrostatics in protein interactions could be investigated explicitly. Cyt$f$ from *P. laminosum*, with a net charge of −14, was used as the partner protein. It is important to note that *P. laminosum* cyt$f$ shares 74 and 72% sequence identity with *Anabaena* cyt$f$ and *S. elongatus* cyt$f$, respectively. Furthermore, the net charge is intermediate of cyt$f$ from *Anabaena* (−16) and *S. elongatus* (−12). This study reports the first structural characterization of the interactions of cyt$f$ and cytc_6.

EXPERIMENTAL PROCEDURES

Protein Preparation—The soluble fragment of cyt$f$ was prepared according to previously published methods (15, 16). Unlabeled *Ana*-cytc_6 was produced in *Escherichia coli* GM119 (17) transformed with both pEAC-WT (18) and pEC86 (19). The culture was grown in LB

[1] The abbreviations used are: PSI, photosystem I; Pc, plastocyanin; cyt$c$, cytochrome c; cytc_6, cytochrome c_6; cyt$f$, cytochrome f; *Ana*, *Anabaena*; *Syn*, *Synechococcus*; HSQC, heteronuclear single quantum correlation spectroscopy; TOCSY, total correlation spectroscopy; NOESY, nuclear Overhauser enhancement spectroscopy.
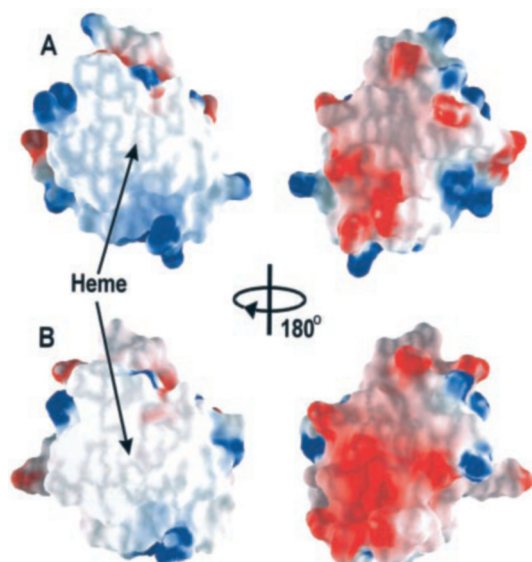
FIG. 1. **Electrostatic potential surfaces of *Ana*-cyt*c*₆ model (*A*) (see "Results and Discussion") and *Syn*-cyt*c*₆ (*B*) (25).** All images were created with a color ramp for positive (*blue*) or negative (*red*) surface potentials saturating at 10 *kT*. Potentials were calculated, for formal charges only, and surfaces were rendered in GRASP (43). The *arrows* indicate the location of the exposed heme edge.
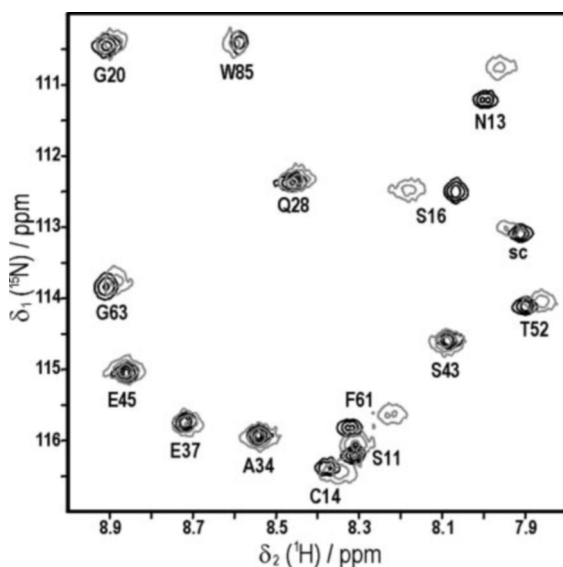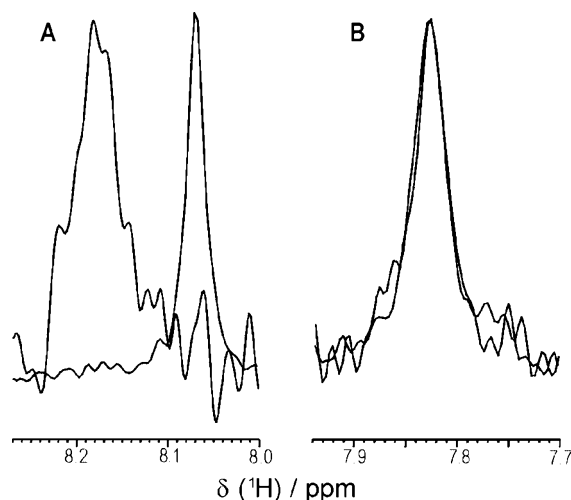

FIG. 3. **Line broadening effects.** *A*, cross-sections along the F_2 dimension through the $^1H^N$ resonance of Ser-16 in *Ana*-cyt*c*₆. The resonance in the free protein (8.07 ppm) has a line width at half-height of 13 Hz. In the presence of two equivalents of cyt*f*, the resonance shifts to 8.18 ppm, and the line width at half-height increases to 34 Hz. *B*, cross-sections along the F_2 dimension through the $^1H^N$ resonance of Gly-12 in *Syn*-cyt*c*₆. Despite the presence of two equivalents of cyt*f*, the resonance is unperturbed (compare Ala-12 of *Ana*-cyt*c*₆, Fig. 4), and the line width at half-height increases by only 2 Hz.
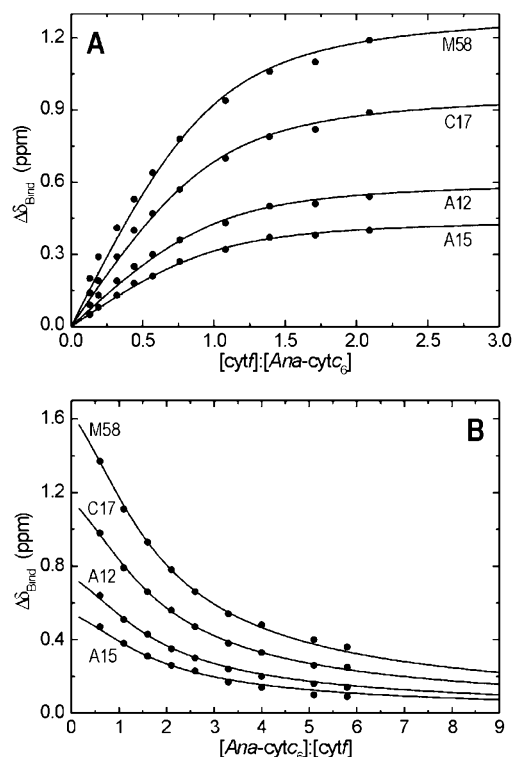

FIG. 2. **Spectral region from overlaid ^1H-^{15}N HSQC spectra of free *Ana*-cyt*c*₆ (*black*) and *Ana*-cyt*c*₆ in the presence of two equivalents of cyt*f* (*gray*).**

FIG. 4. **Binding curves for the interaction of *Ana*-cyt*c*₆ and cyt*f*.** As shown in *A*, a 0.3 mM sample of ^{15}N-*Ana*-cyt*c*₆ was titrated with a 1.9 mM solution of cyt*f*. The data were simultaneously fitted (nonlinear, least-squares) to a 1:1 model (27), yielding a binding constant of $\sim1 \times 10^4$ M^{-1}. As shown in *B*, in the reverse titration, a 0.5 mM sample of cyt*f* was titrated with a 3.0 mM *Ana*-cyt*c*₆ stock. Fits to the 1:1 model yielded a binding constant of 8 (±2) $\times 10^3$ M^{-1}.

medium (20) supplemented with 100 μg/ml ampicillin, 10 μg/ml chloramphenicol, and 1 mM FeCl₃. Aerobic growth was maintained at 37 °C for 18 h before harvesting. A similar expression system in *E. coli* JM109 was used for the production of uniformly ^{15}N-labeled *Ana*-cyt*c*₆. The culture was grown in M9 minimal media additionally supplemented with 1 g/liter $^{15}NH_4Cl$ and 1 mM thiamine. Aerobic growth was maintained at 37 °C for 72 h before harvesting. Isolation and purification of *Ana*-cyt*c*₆ were achieved as described previously (8, 18). The preparation and purification of ^{15}N, ^{13}C double-labeled *Syn*-cyt*c*₆ have been reported previously (21).

NMR Samples—Protein interactions were investigated for the diamagnetic species only, and reducing conditions were maintained in the presence of sodium ascorbate. Protein solutions were concentrated to the required volume using ultrafiltration methods (Amicon; YM3 membrane) and exchanged into 10 mM potassium phosphate, pH 6.0, 10% D₂O, 1.0 mM sodium ascorbate. Protein concentrations were determined spectrophotometrically using an ϵ_{553} of 26.2 mM^{-1}cm^{-1} for the ferrous form of both *Ana*-cyt*c*₆ (22) and *Syn*-cyt*c*₆ and an ϵ_{556} of 31.5 mM^{-1}cm^{-1} for the ferrous form of cyt*f*. For the assignment of *Ana*-cyt*c*₆, 0.7 mM

^{15}N-labeled and 1.0 mM unlabeled samples were prepared. To investigate complex formation between *Ana*-cyt*c*₆ and cyt*f*, microliter aliquots of a 1.9 mM cyt*f* stock solution were titrated into an NMR sample containing 0.3 mM ^{15}N-*Ana*-cyt*c*₆. A reverse titration was also performed in which a sample containing 0.2 mM ^{15}N-*Ana*-cyt*c*₆ and 0.5 mM cyt*f* was titrated with a 3.0 mM stock of unlabeled *Ana*-cyt*c*₆. To investigate complex formation between *Syn*-cyt*c*₆ and cyt*f*, a 0.35 mM sample
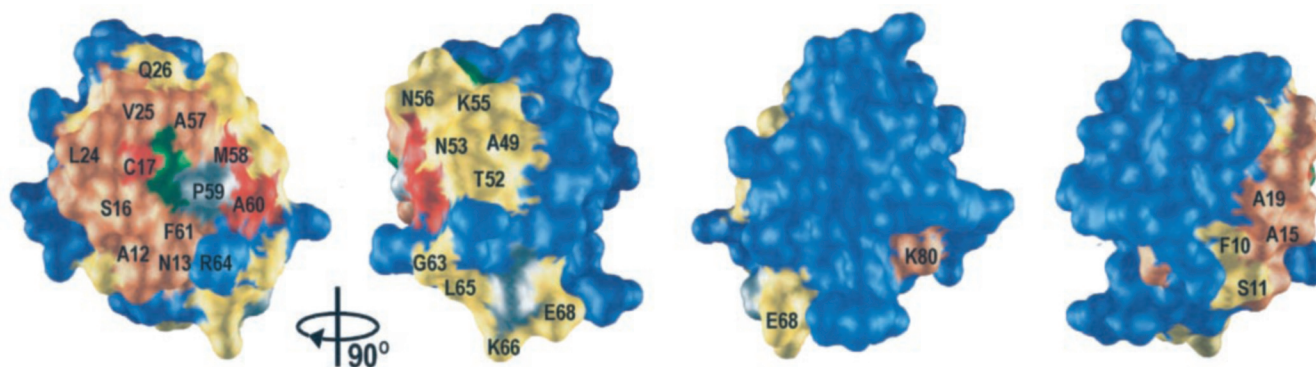
FIG. 5. **Chemical-shift map of *Ana*-cyt*c₆* in the presence of two equivalents of *P. laminosum* cyt*f*.** Residues are *colored* according to their largest $\Delta\delta_{\text{Bind}}$ (ppm): *blue*, < 0.03 (^{1}H) and < 0.1 (^{15}N); *yellow*, ≤ 0.06 (^{1}H) and ≤ 0.3 (^{15}N); *orange*, ≤ 0.10 (^{1}H) and ≤ 0.6 (^{15}N); *red*, ≤ 1.0 (^{1}H) and ≤ 2.0 (^{15}N). Prolines are indicated in *gray*, and the heme is colored *green*. Each view represents a 90° rotation with respect to the previous orientation.

of ^{15}N, ^{13}C-*Syn*-cyt*c₆* was titrated with a 1.9 mM cyt*f* solution. After each addition of protein, the pH of the samples was verified, and ^{1}H-^{15}N HSQC spectra were recorded.

NMR Spectroscopy—For sequence-specific assignment of the backbone resonances of *Ana*-cyt*c₆*, two-dimensional ^{1}H-^{15}N HSQC, three-dimensional ^{1}H-^{15}N NOESY-HSQC (100 ms mixing time), and three-dimensional ^{1}H-^{15}N TOCSY-HSQC (80 ms mixing time) spectra were recorded on a Bruker DRX 500 NMR spectrometer. For assignment of the side-chain protons, two-dimensional homonuclear NOESY and TOCSY spectra were recorded. XWINNMR was used for spectral processing, and the assignment was performed in XEASY (23). Complete assignments of the ^{1}H and ^{15}N resonances were determined for all backbone amides (see Supplementary material, Table S1). The non-exchangeable side-chain protons were also assigned. This assignment is consistent with those reported previously for *Monoraphidium braunii* cyt*c₆* (24) and *Syn*-cyt*c₆* (25).

Measurements on samples containing cyt*f* and either ^{15}N-*Ana*-cyt*c₆* or ^{15}N, ^{13}C-*Syn*-cyt*c₆* were performed on a Bruker DMX 600 NMR spectrometer operating at 300 K. Two-dimensional ^{1}H-^{15}N HSQC spectra (26) were recorded with spectral widths of 30.0 ppm (^{15}N) and 13.9 ppm (^{1}H). Analysis of the chemical-shift perturbation ($\Delta\delta_{\text{Bind}}$) with respect to the free protein was performed in XEASY.

Binding Curves—Titration curves were obtained by plotting $\Delta\delta_{\text{Bind}}$ against the molar ratio (R) of [cyt*f*]:[*Ana*-cyt*c₆*]. For the reverse titration, $\Delta\delta_{\text{Bind}}$ was plotted *versus* [*Ana*-cyt*c₆*]:[cyt*f*]. Non-linear least-squares fits to a one-site model (27) were performed in Origin (Originlab, Northhampton, MA). This model explicitly treats the concentration of both proteins with R and $\Delta\delta_{\text{Bind}}$ as the independent and dependent variables, respectively (27). The binding constant (K_a) and the maximum chemical-shift change ($\Delta\delta_{\text{Max}}$) were the fitted parameters. A global fit was performed in which the curves were fitted simultaneously to a single K_a value, whereas $\Delta\delta_{\text{Max}}$ was allowed to vary for each resonance.

RESULTS AND DISCUSSION

The Complex of cytf and Ana-cytc₆—Comparison of ^{1}H-^{15}N HSQC spectra of free *Ana*-cyt*c₆* and *Ana*-cyt*c₆* in the presence of cyt*f* revealed distinct differences arising from complex formation (Fig. 2). When cyt*f* was titrated into *Ana*-cyt*c₆*, 33 of the backbone amides experienced chemical-shift perturbation, $\Delta\delta_{\text{Bind}} \geq 0.03$ ppm (^{1}H) and/or ≥ 0.10 ppm (^{15}N). A single averaged resonance was observed for each backbone amide, indicating that the free and bound forms of cyt*c₆* were in fast exchange on the NMR time scale. In addition to chemical-shift perturbation, the presence of cyt*f* caused a general broadening of about 20 Hz of the amide resonances (Fig. 3*A*), as expected for complex formation (28).

Titration curves of $\Delta\delta_{\text{Bind}}$ *versus* the molar ratio of cyt*f*:*Ana*-cyt*c₆* were plotted for the ^{15}N nuclei of the four most strongly shifted resonances (Fig. 4*A*). The curves clearly illustrate that the chemical-shift perturbation increases as a function of the cyt*f* concentration. Despite the addition of two equivalents of cyt*f*, however, saturation of the chemical-shift changes was not observed. The binding curves were fitted to a 1:1 model with a

binding constant of $\sim 1 \times 10^4$ M^{-1}. The quality of the fit is poor, particularly at the beginning of the curve, which is perhaps due to a small systematic error in the determination of the protein ratio. To investigate this further, a reverse titration was performed in which a sample of cyt*f* was titrated with *Ana*-cyt*c₆*. In this case, the binding curves were fitted satisfactorily with a binding constant of $8 \ (\pm 2) \times 10^3$ M^{-1} (Fig. 4*B*). It can be concluded that the binding affinity of cyt*f* for *Ana*-cyt*c₆* is $\sim 10^4$ M^{-1}, which is about 2 orders of magnitude greater than the affinity for the physiological partner, *P. laminosum* Pc (15, 29). From the ratio of the observed $\Delta\delta_{\text{Bind}}$ to the fitted $\Delta\delta_{\text{Max}}$ (Fig. 4*B*), it was calculated that 63% of the *Ana*-cyt*c₆* was bound in the first point of the reverse titration.

Six structures of cyt*c₆*, from green algal (30–32), red algal (33), and cyanobacterial (12, 25) sources, have been determined previously. All of the known structures exhibit high structural homology. At present, the structure of *Ana*-cyt*c₆* is unavailable, and therefore, a model was built in Swiss-MODEL (34) using the NMR structure of *Syn*-cyt*c₆* (25) as a template. The chemical-shift map in Fig. 5 illustrates the location of the affected residues in this model with each residue *colored* according to its observed $\Delta\delta_{\text{Bind}}$. The complex interface consists of a well defined patch, which surrounds the exposed methyl groups (methyl 3, thioether 4 methyl, and methyl 5) of the heme. This patch is composed mainly of three stretches of the primary structure, residues 9–19, 23–26, and 51–61. The first of these includes the heme-binding motif C*XY*CH, whereas the sixth ligand, Met-58, occurs in the third stretch. Val-25, which was shown to be important for the interaction between cyt*c₆* and PSI (8), is found in the second stretch. Cys-17, Met-58, and Ala-60 experience the largest shifts in the complex. Alanine and asparagine are the most abundant residues in the interface, accounting for one-third of all the affected residues. Although 60% of the interface can be classified as hydrophobic, only 4 residues are charged (Lys-55, Lys-66, Glu-68, and Lys-80). Notably the conserved arginine, Arg-64, which has been implicated in the reaction with PSI (9), was not shifted in the complex. Fragata (35) has produced a theoretical model of the complex formed between *M. braunii* cyt*c₆* and turnip cyt*f* (Protein Data Bank accession code 1jx8). There is good agreement between the binding site on cyt*c₆* identified in this model and the experimentally observed interaction site on *Ana*-cyt*c₆*.

The complex of cyt*f* and *Ana*-cyt*c₆* was also investigated at 50, 100, and 200 mM NaCl. The observed $\Delta\delta_{\text{Bind}}$ for the 33 affected amides is plotted as a function of the salt concentration in Fig. 6. As the salt concentration was increased, $\Delta\delta_{\text{Bind}}$ decreased. At 200 mM NaCl, the $\Delta\delta_{\text{Bind}}$ is zero for most residues. This suggests that the binding constant is considerably re-
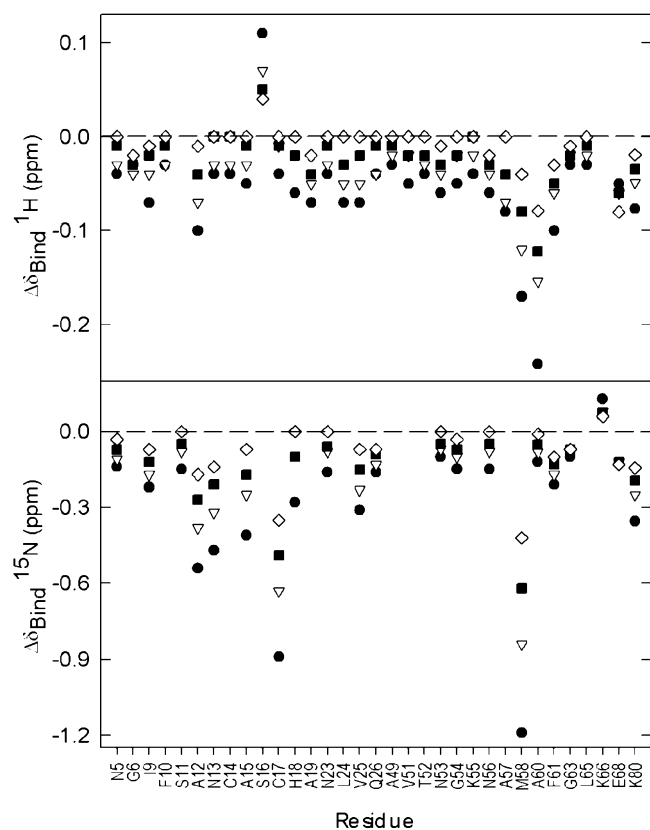
FIG. 6. **Salt dependence of $\Delta\delta_{Bind}$ for all 33 affected backbone amide resonances, observed in the complex of *Ana*-cytc_6 and cyt$f$ at 0 mM NaCl ($\bullet$), 50 mM NaCl ($\triangledown$), 100 mM NaCl ($\blacksquare$). and 200 mM NaCl ($\diamond$).**

FIG. 7. **Comparison of the chemical-shift maps of yeast cyt$c$ (29) (A) and *Ana*-cytc_6 (B) in the presence of cyt$f$, with *color coding* as in Fig. 5.** The experimentally ranked docking solutions generated by BiGGER (42) are illustrated in the *lower panel*. Cyt$f$ is depicted as the C^a trace with the heme group in spacefill. The geometric centers of cyt$c$ (C) and *Ana*-cytc_6 (D) are represented by *spheres* in each of the top 50 docking orientations. *Color coding* from *green* to *red* indicates the ranking position, with *red* being more favorable.

duced, illustrating the importance of attractive electrostatic interactions in complex formation. The more strongly affected residues such as Cys-17 and Met-58 still experience appreciable shifts at 200 mM NaCl. Furthermore, although the line broadening decreased with increasing salt, there remains ~5 Hz broadening at 200 mM NaCl. These observations are indicative of a significant interaction even at high ionic strength.

The Interactions of cytf and Syn-cytc₆—In contrast to the case of *Ana*-cytc_6, titration of cyt$f$ into *Syn*-cytc_6 produced only minor effects in the ¹H-¹⁵N HSQC spectra. Despite the presence of two equivalents of cyt$f$, the amide resonances of *Syn*-cytc_6 did not experience chemical-shift perturbation. Line broadening effects on the order of 2 Hz were observed (Fig. 3B), consistent with a weak and highly dynamic interaction (36). Increasing the ionic strength by the addition of 200 mM NaCl had no effect on the protein interactions. In contrast to the clearly defined complex between cyt$f$ and *Ana*-cytc_6, there is no evidence for specific complex formation with *Syn*-cytc_6.

Biological Implications—From our results, it is clear that *Ana*-cytc_6 and cyt$f$ form a well defined complex and that the amount of complex formed is dependent on the ionic strength. It has been shown previously that *Ana*-cytc_6 forms a complex with *Anabaena* PSI, the affinity of which decreases with increasing ionic strength (7). Although *Ana*-cytc_6 has a net charge close to zero, the presence of positive residues in the vicinity of the heme group promotes favorable electrostatic docking to cyt$f$. The role of electrostatics in this complex is therefore analogous to the complex formed between plant cyt$f$ and Pc *in vitro* (14, 27, 37–39). As illustrated in Fig. 5, the interaction site of *Ana*-cytc_6 is composed mainly of hydrophobic residues, which is necessary to achieve specific complex formation between the two proteins. Such a hydrophobic site is sim-
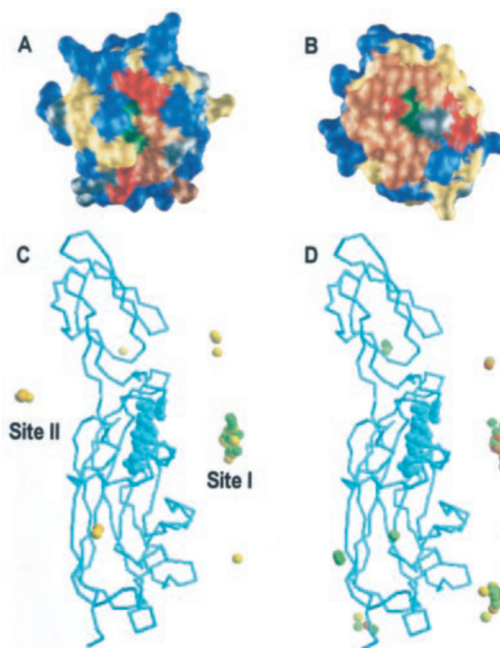
ilar to that proposed previously for the interaction of *Ana*-cytc_6 with PSI (8).

A type I mechanism has been reported for the reduction of PSI by *Syn*-cytc_6 (21). In this mechanism, the electron transfer rate is proportional to the number of collisions in which the redox centers of both proteins are aligned. The NMR titration of cyt$f$ into *Syn*-cytc_6 provides no evidence for specific complex formation but suggests a highly dynamic interaction between these partners, in agreement with a type I mechanism. The optimal orientation for productive collisions is facilitated by the prominent acidic patch on the backside of *Syn*-cytc_6 (Fig. 1) since the front face will be the energetically more favorable approach with the acidic partners, cyt$f$ and PSI. Apparently, cytc_6 from different organisms utilizes different mechanisms for the electron transfer reaction with its partners. A similar conclusion has been reached for the interactions of cyt$f$ and Pc from different organisms (15). The source of this different reactivity can be traced to the nature of the protein surfaces and ultimately to variations in the primary structures. The sequences of *Ana*-cytc_6 and *Syn*-cytc_6 share 67% identity. Of the 33 residues identified in the *Ana*-cytc_6 interaction site, 22 are conserved in the *Syn*-cytc_6 sequence. Only 6 residues, located around the periphery of the complex interface, are significantly different in *Syn*-cytc_6. Ala-19 and Gln-26 are replaced by methionines, which have been implicated as endogenous antioxidants (25, 40). Ala-49 is replaced by a tyrosine, whereas glutamine and histidine replace Thr-52 and Asn-53, respectively. This cluster of three variations in *Syn*-cytc_6 results in a bulkier surface, which may hinder interactions with cyt$f$. The replacement of Lys-66 by a threonine in *Syn*-cytc_6 is representative of the most striking difference between the two sequences. Five additional lysines in *Ana*-cytc_6 contribute to the significantly higher pI of this protein and enable attractive electrostatic interactions with the acidic cyt$f$.

The different roles of electrostatics and hydrophobics can be

further illustrated by comparison with the recently characterized, non-physiological complex of yeast cytochrome *c* (cyt*c*) and cyt*f* (29). It was found that cyt*f* binds two equivalents of cyt*c* with binding constants of $\sim 2 \times 10^4$ M^{-1} and 4×10^3 M^{-1}. The higher binding affinity, as compared with the cyt*f*-*Ana*-cyt*c*$_6$ complex, probably arises from the strong electrostatic attraction between cyt*f* and cyt*c*, which has a pI of 9.7 (41). Fewer residues experienced chemical-shift perturbation in this complex, resulting in a less extensive interaction site (29) (Fig. 7, *A* and *B*). Furthermore, the chemical-shift perturbation was on average 50% smaller than that observed in the complex with *Ana*-cyt*c*$_6$. The prevalence of electrostatic attractions may reduce the amount of time spent in a single orientation, as determined by hydrophobic contacts, and consequently, fewer and smaller chemical-shift changes are observed. Alternatively, the diminished interaction site observed for cyt*c* may be explained in terms of "goodness of fit." It can be assumed that the hydrophobic patch surrounding the heme is better adapted in *Ana*-cyt*c*$_6$ than in yeast cyt*c* for binding to cyt*f*. This complimentarity favors closer contact between the protein surfaces and thus a larger interaction site.

Protein docking simulations, using an NMR filter implemented in BiGGER (42), identified the cyt*c* binding sites as the front (Site I) and back (Site II) faces of the heme region of cyt*f* (29) (Fig. 7*C*). A similar docking simulation using the *Ana*-cyt*c*$_6$ model gave slightly different results. Although the front face of the heme remains the favored site of interaction, there is a significant fraction of favorable docking orientations beneath the heme region in the large domain of cyt*f* (Fig. 7*D*). Notably, there is significant overlap between the top-ranking docking configuration found for *Ana*-cyt*c*$_6$ in BiGGER and the docking orientation of *M. braunii* cyt*c*$_6$ in the model of Fragata (35). In this model, between the algal cyt*c*$_6$ and plant cyt*f*, there are favorable electrostatics between complimentary charged patches, a ridge of lysines on the small domain of cyt*f* and a cluster of acidic residues on the side of cyt*c*$_6$. This results in a slightly different orientation of cyt*c*$_6$ in comparison with the cyanobacterial complex, which does not possess such well defined complimentary charged patches.

REFERENCES

1. Wood, P. M., (1978) *Eur. J. Biochem.* **87,** 9–19
2. Wastl, J., Bendall, D. S., and Howe, C. J. (2002) *Trends Plant Sci.* **7,** 244–245
3. Gupta, R., He, Z. Y., and Luan, S. (2002) *Nature* **417,** 567–571
4. Navarro, J. A., Hervás, M., and De la Rosa, M. A. (1997) *J. Biol. Inorg. Chem.* **2,** 11–22
5. Kerfeld, C. A., and Krogmann, D. W. (1998) *Annu. Rev. Plant Physiol.* **49,** 397–425
6. Hervás, M., Navarro, J. A., Díaz, A., Bottin, H., and De la Rosa, M. A. (1995) *Biochemistry* **34,** 11321–11326
7. Hervás, M., Navarro, J. A., Díaz, A., and De la Rosa, M. A. (1996) *Biochemistry* **35,** 2693–2698
8. Molina-Heredia, F. P., Díaz-Quintana, A., Hervás, M., Navarro, J. A., and De la Rosa, M. A. (1999) *J. Biol. Chem.* **274,** 33565–33570
9. Molina-Heredia, F. P., Hervás, M., Navarro, J. A., and De la Rosa, M. A. (2001) *J. Biol. Chem.* **276,** 601–605
10. Hippler, M., Drepper, F., Haehnel, W., and Rochaix, J. D. (1998) *Proc. Natl. Acad. Sci. U. S. A.* **95,** 7339–7344
11. Illerhaus, J., Altschmied, L., Reichert, J., Zak, E., Herrmann, R. G., and Haehnel, W. (2000) *J. Biol. Chem.* **275,** 17590–17595
12. Frazão, C., Soares, C. M., Carrondo, M. A., Pohl, E., Dauter, Z., Wilson, K. S., Hervas, M., Navarro, J. A., De la Rosa, M. A., and Sheldrick, G. M. (1995) *Structure* **3,** 1159–1169
13. Ullmann, G. M., Hauswald, M., Jensen, A., Kostic, N. M., and Knapp, E. W. (1997) *Biochemistry* **36,** 16187–16196
14. Ubbink, M., Ejdeback, M., Karlsson, B. G., and Bendall, D. S. (1998) *Structure* **6,** 323–335
15. Crowley, P. B., Otting, G., Schlarb-Ridley, B. G., Canters, G. W., and Ubbink, M. (2001) *J. Am. Chem. Soc.* **123,** 10444–10453
16. Schlarb, B. G., Wagner, M. J., Vijgenboom, E., Ubbink, M., Bendall, D. S., and Howe, C. J. (1999) *Gene* (*Amst.*) **234,** 275–283
17. Marinus, M. G., and Morris, N. R. (1973) *J. Bacteriol.* **14,** 1143–1150
18. Molina-Heredia, F. P., Hervás, M., Navarro, J. A., and De la Rosa, M. A. (1998) *Biochem. Biophys. Res. Commun.* **243,** 302–306
19. Arslan, E., Schulz, H., Zufferey, R., Künzaler, P., and Thöny-Meyer, L. (1998) *Biochem. Biophys. Res. Commun.* **251,** 744–747
20. Sambrook, J., Fritsch, E. F., and Maniatis, T. (1989) *Molecular Cloning: A Laboratory Manual,* 2nd Ed., Cold Spring Harbor Laboratory, Cold Spring Harbor, NY
21. Sutter, M., Sticht, H., Schmid, R., Hörth, P., Rösch, P., and Haehnel, W. (1995) in *Photosynthesis: From Light to Biosphere* (Mathis, P. ed.), Vol. II, pp. 563–566, Kluwer Academic Publishers, The Netherlands,
22. Medina, M., Louro, R. O., Gagnon, L., Peleato, M. L., Mendes, J., Gómez-Moreno, C., Xavier, A. V., and Teixeira, M. (1997) *J. Biol. Inorg. Chem.* **2,** 225–234
23. Bartels, C., Xia, T.-H., Billeter, M., Güntert, P., and Wüthrich, K. (1995) *J. Biomol. NMR* **5,** 1–10
24. Banci, L., Bertini, I., De la Rosa, M. A., Koulougliotis, D., Navarro, J. A., and Walter, O. (1998) *Biochemistry* **37,** 4831–4843
25. Beißinger, M., Sticht, H., Sutter, M., Ejchart, A., Haehnel, W., and Rösch, P. (1998) *EMBO J.* **17,** 27–36
26. Andersson, P., Gsell, B., Wipf, B., Senn, H., and Otting, G. (1998) *J. Biomol. NMR* **11,** 279–288
27. Kannt, A., Young, S., and Bendall, D. S. (1996) *Biochim. Biophys. Acta-Bioenergetics* **1277,** 115–126
28. Zuiderweg, E. R. P. (2002) *Biochemistry* **41,** 1–7
29. Crowley, P. B., Rabe, K. S., Worrall, J. A. R., Canters, G. W., and Ubbink, M. (2002) *ChemBioChem* **3,** 526–533
30. Kerfeld, C. A., Anwar, H. P., Interrante, R., Merchant, S., and Yeates, T. O. (1995) *J. Mol. Biol.* **250,** 627–647
31. Schnackenberg, J., Than, M. E., Mann, K., Wiegand, G., Huber, R., and Reuter, W. (1999) *J. Mol. Biol.* **290,** 1019–1030
32. Yamada, S., Park, S.-Y., Shimizu, H., Koshizuka, Y., Kadokura, K., Satoh, T., Suruga, K., Ogawa, M., Isogai, Y., Nishio, T., Shiro, Y., and Oku, T. (2000) *Acta Crystallogr. Sect. D Biol. Crystallogr.* **56,** 1577–1582
33. Sawaya, M. R., Krogmann, D. W., Serag, A., Ho, K. K., Yeates, T. O., and Kerfeld, C. A. (2001) *Biochemistry* **40,** 9215–9225
34. Guex, N., and Peitsch, M. C., (1997) *Electrophoresis* **18,** 2714–2723
35. Fragata, M. (2002) *Biophys. J.* **82,** 1618
36. Worrall, J. A. R., Liu, Y., Crowley, P. B., Nocek, J. M., Hoffman, B. M., and Ubbink, M. (2002) *Biochemistry* **41,** 11721–11730
37. Soriano, G. M., Ponamarev, M. V., Piskorowski, R. A., and Cramer, W. A. (1998) *Biochemistry*, **37,** 15120–15128
38. Bergkvist, A., Ejdeback, M., Ubbink, M., and Karlsson, G. (2001) *Protein Sci.* **10,** 2623–2626
39. Soriano, G. M., Ponamarev, M. V., Tae, G.-S., and Cramer, W. A. (1996) *Biochemistry*, **35,** 14590–14598
40. Levine, R. L., Mosoni, L., Berlett, B. S., and Stadtman, E. R. (1996) *Proc. Natl. Acad. Sci. U. S. A.* **93,** 15036–15040
41. Park, K. S., Frost, B. F., Shin, S., Park, I. K., Kim, S., and Paik, W. K. (1988) *Arch. Biochem. Biophys.* **267,** 195–204
42. Palma, P. N., Krippahl, L., Wampler, J. E., and Moura, J. J. G. (2000) *Proteins* **39,** 372–384
43. Nicholls, A., Sharp, K., and Honig, B. (1991) *Proteins* **11,** 281–296